

INVESTIGATION OF STRUCTURAL, MAGNETIC AND ELECTRICAL PROPERTIES OF PURE LaFeO_3 SYNTHESIZED THROUGH SOLUTION COMBUSTION TECHNIQUE

P. JAIN*, S. SRIVASTAVA

Materials Science & Metallurgical Engineering, Maulana Azad National Institute of Technology, Bhopal-462003, India

Lanthanum ferrite (LFO), perovskite-type oxide was prepared by solution combustion method using acetylacetone as chelating agent and urea as fuel. Differential thermal analysis (DTA) and thermogravimetric analysis (TGA) used to investigate the mechanism of various reactions involved in the process. Structural parameters such as atomic positions, bond angle and lattice parameters were calculated by Rietveld refinement of XRD data. Further, the SEM and EDAX study was carried out to analyze the surface morphology and elemental composition, respectively. The magnetic behaviour was observed by vibrating sample magnetometer (VSM). The temperature dependence conductivity measurements were done to evaluate the activation energy (E_a). The present study underlines the influence of structure and morphology (porosity) of LFO on magnetization at room temperature and also observed the effect of temperature on its insulating behaviour.

(Received December 1, 2015; Accepted February 5, 2015)

Keywords: Pervoskite; Solution combustion; X-ray analysis; Magnetic properties

1. Introduction

Multiferroics are the key materials which exhibit ferroelectric and magnetic properties in a single phase, which are extensively rare from those of conventional materials. There are various such materials are present like BiFeO_3 , BiMnO_3 , and DyFeO_3 [1-3]. Despite having different attractive features, they concern some serious drawback of leakage current caused by oxygen and /or cation vacancies and secondary impurities [4]. Therefore, it is crucial to develop new alternative materials that open the novel opportunity for the device fabrication, sensors and next generation storage media [5].

Recently, LaFeO_3 has received enormous attention due to its multiferrocity [6]. In addition to this multiferrocity, it possesses high thermal stability and well defined structure. These intriguing properties have been providing one more degree of freedom for utilization in a number of advanced technologies across the worldwide. In general, LaFeO_3 shows G-type weak antiferromagnetic ordering below 735 K and ferroelectric transition at 475 K [7]. It comes under the classes of rare-earth orthoferrites (ABO_3) with a space group Pbnm , here BO_6 octahedra rotates, while the Fe^{+3} cation slightly shifts from their centrosymmetric position. Therefore, the displacement of the A ion with BO_6 octahedra cause ferroelectricity and Fe-O-Fe super exchange interaction leading to the canted antiferromagnetic ordering in the system.

In the preparation of the oxide based ceramics generally the time and temperature play a crucial role in the formation of high quality material. An excess temperature always promotes grain growth rapidly leading to the agglomeration of grains is observed and lower temperature stays chemical reaction incomplete, because the low mobility of the constituent ions. Even the

*Corresponding author: pranatjain@gmail.com

optimized temperature and time duration could prevent material from the phase transformation as well as formation of other phases. The conventional oxide based reactions are the most common and inexpensive techniques to prepare single phase perovskite ceramics. Literature reported that [8] these techniques exhibit some limitations; mainly its starting materials are oxides which require several hours of intermediate grinding and high temperature annealing. The pure LFO ceramics were prepared using a solution combustion synthesis. This technique has attracted enormous attention as to it offers self-sustained reaction of the oxidizers (metal nitrates) and fuels that make it simple, versatile and rapid process. This process involves two major steps, which drive the propagation of the reaction. Firstly, the formation of a homogeneous solution of precursor in liquid state is providing atomic level compositional uniformity throughout the reaction, without any precipitation. Secondly, auto-ignition that provides fast heating which helps in the formation of the desired crystalline phase in short duration of intervals. In the present communication, LFO was prepared through solution combustion synthesis and the structural, magnetic and electrical properties of LaFeO₃ are studied.

2. Experimental

The single phase LaFeO₃ sample was prepared by solution combustion synthesis with urea (fuel). The stoichiometric amount of high purity ferric nitrate, lanthanum nitrate, 2-methoxyethanol (C₃H₈O₂) and acetylacetone (C₅H₈O₂) were taken as starting ingredient. The 2-Methoxy ethanol was used as solvent that provide media for synthesis. The metal nitrates were discretely dissolved in small amount of 2-methoxy ethanol and mixed together under constant stirring. Then a few drops of acetylacetone used as a chelating agent was added. The role of chelating agent was to form stable metal-chelate complex that hindered the aggregation of different metal ions in the solution [9]. This approach provides an extra degree of freedom in the formation of homogeneous solution. At last, urea (with calculated fuel-to-oxidizers ratio) was added to the solution [10]. Then solution was introduced into the muffle furnace maintained at 500°C which produced fast and self-ignite redox reaction. Thereafter the bluffly dark yellow powder was obtained. The resultant powder was grounded and calcined at 700°C and 800°C for 3 hrs in a muffle furnace. Then the powder pressed into pellets and sintered at 1300°C for 6 hrs. The heating and cooling rate were maintained at 5°C/min.



The simultaneous analysis from thermogravimetry and differential thermal analysis (TG/DTA) of mixed precursor were performed using a Thermal Analyzer (Melter Toledo). The phase purity and crystal structure were analyzed by using X-ray diffractometer (Bruker D8 Advance) equipped with a CuK α target of ($\lambda=1.54\text{\AA}$) radiation. The Rietveld refinement of the XRD peaks was performed through Fullproff Suit program 2.05. The surface morphology of the pellet was observed by FE-SEM (Carl ZEISS-SUPRA) meanwhile, the subsequently elemental analysis was done by the EDAX detector attached with the FE-SEM. The magnetic measurement was done by a vibrating sample magnetometer (VSM 736, Lake Shore Cryotronics). The conductivity of the LFO was measured using an Alpha high resolution impedance analyzer using Nova Control.

3. Results and discussions

3.1 Thermal behavior

Fig.1 Shows the DTA/TGA curve of precursors of mixed powder. Three stages are observed during the weight loss and energy change in the process from room temperature to 500°C as mentioned in the Fig. 1. The two endothermic peaks present in the graph at 47.8°C and 171.6°C.

Mostly, the endothermic peaks are the signature of loss of water and inorganic residues left during the process of combustion. In the first stage, the weight loss of 30% with first endothermic peak is observed due to the evaporation of physisorbed water [11]. In the second stage, the endothermic peak around 171°C with corresponding weight change of 20% represents the loss of chemisorbed water [12]. At the final stage, the next 20% weight loss in this process indicates starting of the decomposition of nitrates and other gaseous elements [13]. This observation signifies that the reaction between the precursors is very fast. After that no further weight loss was observed. It was clearly found that to obtain the pure LFO; the as-synthesized sample needs to be calcined at above 600°C.

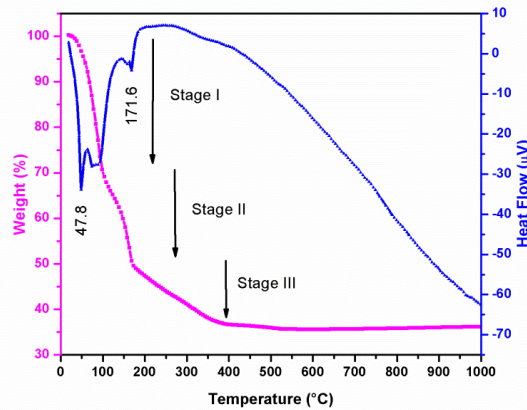


Fig. 1: The DTA/TGA graph of mixed precursors

3.2 XRD analysis

Fig. 2 Shows the XRD patterns of the LFO powders synthesized by solution combustion method. Both the diffraction patterns match with the JCPDS card No. 01-074-2203. As the calcinations, temperature increases the material goes towards crystallization as clearly indicated in the Fig. 2. All the peaks pointed out orthorhombic structure corresponding to Pbnm space group. No extra peaks were observed up to XRD limit. Therefore, we can ensure that the formed material is pure LFO. The crystallite size of LFO samples was estimated through peak broadening β_D of XRD pattern [14].

$$\beta_D^2 = \beta_{Measured}^2 - \beta_{Instrumental}^2$$

The Debye-Scherrer's equation,

$$t = \frac{0.9\lambda}{\beta_D} \cos\theta$$

Where, t is the particle size (nm), $\lambda = 1.5406 \text{ \AA}$ (characteristic CuK_α wavelength of X-rays) and β_D is the peak width at half maximum intensity for peak position 2θ . Pure Si has been taken as a standard for the calculation of instrument broadening. The obtained average crystallite size of the LFO particles is 157.51 nm. The Rietveld refinement was carried to investigate the various structural parameters for the LFO sample. Fig. 3 represents the experimental values, calculated values and its difference with respect to Bragg's position. It is concluded from the fitting parameters that, the structure is very well fitted for orthorhombic system. The χ^2 , R_{Bragg} , R_F and lattice parameter were obtained through calculation and summarized in the table I. The percentage porosity of the sample was calculated using X-ray density from the relation [15].

$$\text{porosity (\%)} = \frac{D_{theoretical} - D_{experimental}}{D_{theoretical}} \times 100$$

Where, $D_{\text{theoretical}}$ and $D_{\text{experimental}}$ are the experimental and theoretical density, respectively. The experimental density of the sintered pellet was measured through the Archimedes technique [16]. After calculating, the percentage porosity of the sample obtained was 9.95 %.

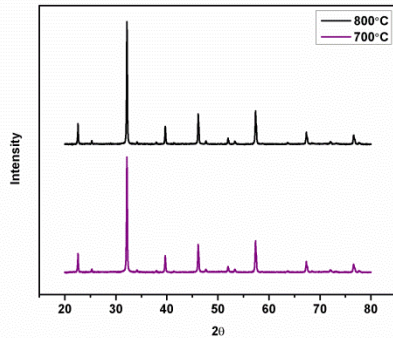


Fig. 2: The XRD graph of LaFeO_3

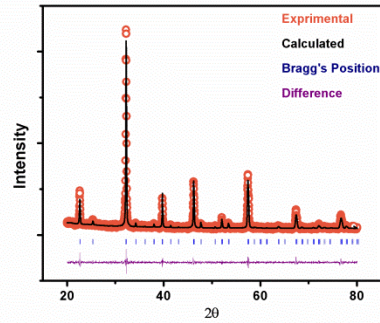


Fig. 3: The Rietveld refinement of LaFeO_3

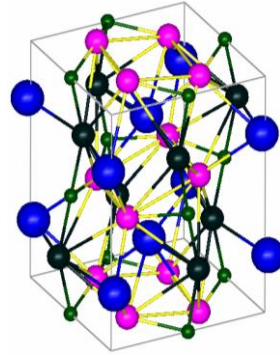


Fig. 4. The orthorhombic structure of the LaFeO_3 unit cell.
The color represents: Blue (La), Green (Fe), Black (O1) and Pink (O2)

Table 1: XRD parameters

		Atomic positions			Bond length (Å°)	Lattice Parameter (Å°) and Volume (Å°) ³	Other parameters
		X	Y	Z			
4c	La	-0.00614	0.02840	0.2500	La-O 3.1582	a=5.5560, b=5.5578	$\chi^2=1.33$
4b	Fe	0.0000	0.5000	0.000	Fe-O 2.0063	c=7.8496	$R_F=3.88$
4c	O1	0.07310	0.48750	0.2500	O-O 2.8675	V=242.390	$R_{\text{Bragg}}=3.05$
8d	O2	-0.28090	0.28150	0.3940		Density= 6.652 g/cm ³	

3.3 SEM analysis

The surface morphology of LFO sintered pellet through field emission scanning electron microscopy (FE-SEM) is shown in the Fig. 5 (a). The LFO sample shows the uniform porosity and homogeneous grain growth throughout the sample. It is well known fact that the formation of porosity is due to insufficient sintering time and/or temperature, which results in an inadequate grain growth and density. The average grain size of LFO is found to be 0.377 μm . The size of these grains was estimated through the grain size distribution graph as shown in fig. 5 (b). The chemical composition of the LaFeO_3 was analyzed through energy dispersive x-ray spectroscopy (EDAX) as shown in the Fig. 5 (c), which represents that all the elements (La, Fe and O) were present nearly in the proper ratio throughout the sample.

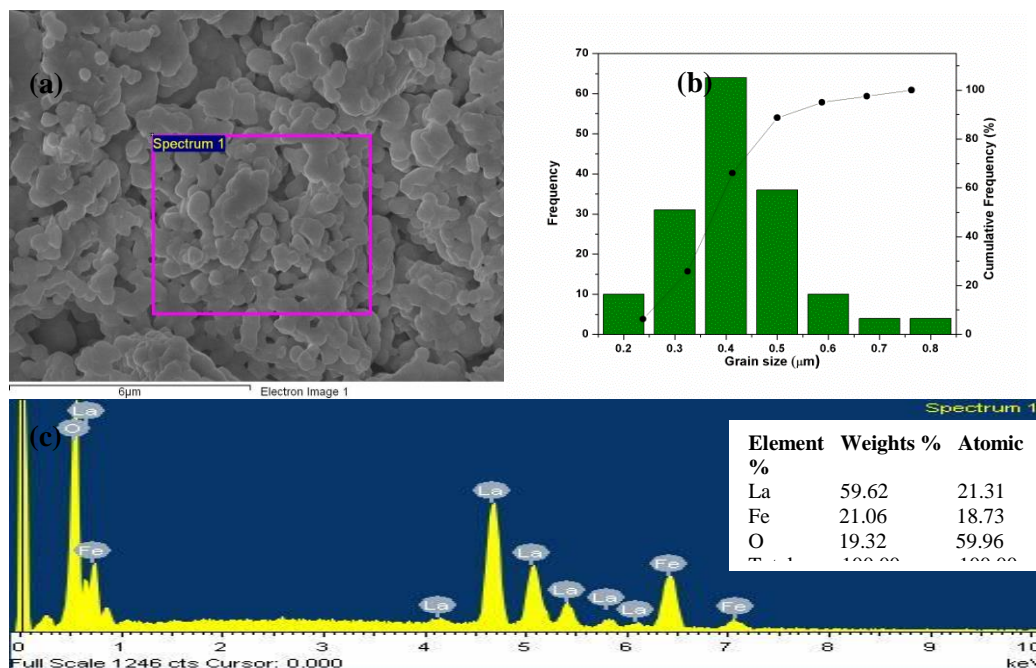


Fig. 5. (a) The SEM image of LaFeO_3 calcined at 800°C ; (b) The Particle size distribution graph of LaFeO_3 ; (c) EDAX

3.4 Magnetic measurements

The magnetization curve (M-H) at the room temperature of the LaFeO_3 pellets sintered at 1300°C is shown in the Fig. 7. In brief, the curve displays no saturation within the range of applied magnetic field. The magnetization curve indicates nearly zero remnant magnetization and low coercive field of 1867 Oe. This represents antiferromagnetic ordering of the Fe^{+3} spin [17]. The reason behind the origin of weak magnetization in the present case of LFO may be due to the grain morphology. However, sintering alters the grain growth, which affects the structural and magnetic disorders in the materials. The SEM image and density measurement results show that, the porosity of the material is affected on the magnetization of the materials. Kadam et al [18] studied LaFeO_3 ceramics synthesized by Sol-gel auto combustion method and reported 435.06 Oe of coercive field for 26.1% of porosity at the room temperature. Therefore, the value of coercive magnetization is strongly influenced by the size of the pores in the materials [19].

In addition to that, LaFeO_3 is known to have weak magnetic material similar to other Bi- and Y-orthoferrites [20, 21]. The interaction of transition-metal ions (here Fe^{3+}) spin via oxygen ion leading to spin canting phenomenon due to exchange coupling generates a very less net magnetic moment in the materials [22].

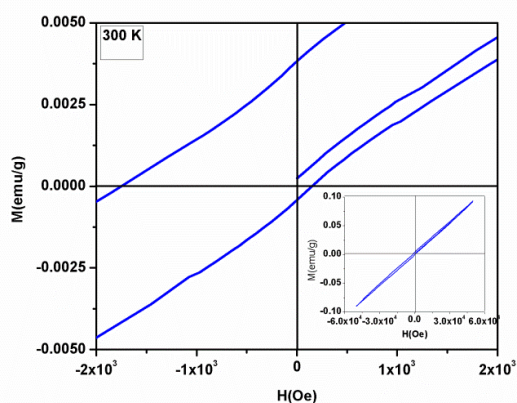


Fig. 7. (a) The magnetic field Vs magnetization for LaFeO_3

3.5 Conductivity measurements

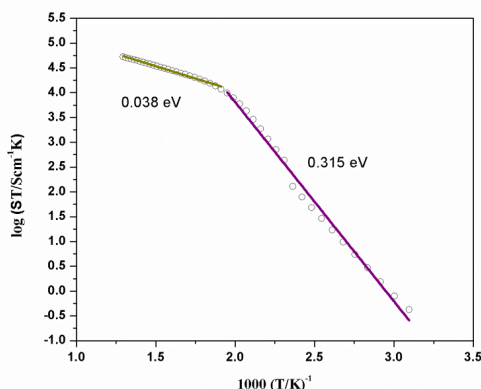


Fig. 8. Conductivity as a function of temperature

Fig. 8 shows the dependence of the AC electrical conductivity (σ_{ac}) on temperature (T) of LaFeO₃ ceramic. It is clearly observed from the results that conductivity increases abruptly from RT to 526 K and becomes linear above 526 K with an increase in the temperature. The observed trend is suggested that the conduction process obeys the Arrhenius relationship [23]

$$\sigma = \sigma_0 \exp \left[-\frac{E_a}{KT} \right]$$

Where, σ_0 and k are pre-exponential factor and the Boltzmann constant respectively. From the above equation, the values of activation energy 0.315 eV in the temperature range of RT to 526 K and 0.038 eV beyond 526 K were evaluated. The activation energy (E_a) was found higher at low temperature and lower at high temperature. The pure La based perovskite materials are good insulators at low temperatures and shows insulator to metal transition at high temperature. The observed results are in good agreement with previously reported [24].

4. Conclusion

In summary, the LaFeO₃ ceramic has been successfully prepared using simple and fast solution combustion method using metal nitrates and urea as a fuel. X-ray diffraction results reveal that the pure phase formed at 800°C and exhibit orthorhombic structure with Pbnm space group. The 9.91 % porosity and homogeneous microstructure with 0.377 μm grain size was obtained. The magnetic measurement represents the antiferromagnetic nature and coercive field (H_C) 1867 Oe of the sintered sample at room temperature. The magnetic characterization indicated that the porosity strongly affects the magnetization in the material at room temperature. The observed temperature dependence conductivity measurements show insulator to metal transition at higher temperature. Further studies are needed to use these properties in practical applications.

Acknowledgments

The authors would like to thanks Dr. Mukul Gupta (IUC-UGC-DAE Consortium, Indore) for XRD measurements, Rajan Singh and Baidyanath Sahu from IIT, Bombay for helpful discussions. The authors gratefully acknowledge to MANIT, Bhopal for providing financial support.

References

- [1] Pittala Suresh, S. Srinath, *Journal of Alloys and Compounds*, **554**, 271 (2013).
- [2] Alok Sharan, James Lettieri, Yunfa Jia, Wei Tian, Xiaoqing Pan, Darrell G. Schlom, Venkatraman Gopalan, *Physical Review B* **69**, 1341 (2004).
- [3] Yi Du, Zhenxiang Cheng, Xiaolin Wang, S X. Dou, *Journal of Applied Physics* **107**, 09 (2010).
- [4] G. Catalan, J.F. Scott, *Advanced Material*. **21**, 2463 (2009).
- [5] Irshad Bhat, Shahid Husain, Wasi Khan, S.I. Patil, *Materials Research Bulletin* **48**, 4506 (2013).
- [6] S. Acharya a, J. Mondal a, S. Ghosh b, S.K. Roy b, P.K. Chakrabarti, *Materials Letters* **64**, 415 (2010).
- [7] M. Idrees a,b, M. Nadeem a, M. Atifc, M. Siddique d, M. Mehmood b, M.M. Hassan, *Acta Materialia* **59**, 1338 (2011).
- [8] J. Silva, A. Reyes, H. Esparza, H. Camacho and L. Fuentes, *Integrated Ferroelectrics: An International Journal* **126**(1), 47(2011).
- [9] N. A. Abdullah, N. Osman, S. Hasan, O.H. Hassan, *International Journal of Electrochemical Science* **7**, 9401 (2012).
- [10] S R Jain, K C Adiga, and V R Paiverneker, *Combustion and Flame* **40**, 71 (1981).
- [11] Md. Jakir Hossana, M. A Gafurb, M. R Kadirb and Mohammad Mainul Karima, *International Journal of Engineering & Technology* **14**, No: 01 (2014).
- [12] P. Psuja, D. Hreniak, W. Strek, 2nd National Conference on Nanotechnology 'NANO 2008', *Journal of Physics: Conference Series* **146**, 012033 (2009).
- [13] S. Biamino, C. Badini, *Journal of the European Ceramic Society* **24**, 3021 (2004).
- [14] VD Mote, Y Purushotham and BN Dole, *Journal of Theoretical and Applied Physics* **6**, 6 (2012).
- [15] M.R. Kadam, R.P. Patil, *Solid State Sciences* **14**, 964 (2012).
- [16] Rajan Singh, A.R. Kulkarni, C.S. Harendranath, *Physica B* **434**, 139 (2014).
- [17] M.A. Ahmed, N. Okasha, *Journal of Alloys and Compounds* **553**, 308 (2013).
- [18] M.R. Kadam, R.P. Patil, P.P. Hankare, *Solid State Sciences* **14**, 964 (2012).
- [19] M.P. Bogadanovich, N.G. Eadeeva, A.N. Men, *Izvestiya, akad. nauk, USSR, Neorg. Mater.* **14** 1978).
- [20] Qiang Zhang, Xiaohong Zhu, Yunhui Xu, Haobin Gao, Yunjun Xiao, Dayun Liang, Jiliang Zhu, Jianguo Zhu, Dingquan Xiao, *Journal of Alloys and Compounds* **546**, 57 (2013).
- [21] Hui Shen, Jiayue Xu, Anhua Wu, Jingtai Zhao, Minli Shi, *Materials Science and Engineering B* **157**, 77 (2009).
- [22] Zavaliche, A. P. Shafer, R. Ramesh, M. P. Cruz, R. R. Das, D. M. Kim, C. B. Eom, *Applied Physics Letters* **87**, 252 (2005).
- [23] Ajay Kumar Behera, Nilaya K. Mohanty, Banarji Behera, Pratibindhya Nayak, *Advanced Materials Letters* **4**(2), 141 (2013).
- [24] Refka Andoulsi, Karima Horchani-Naifer, Mokhtar Férid, *Powder Technology* **230**, 183 (2012).